

PHYSICAL PARAMETERS OF GRB 970508 AND GRB 971214 FROM THEIR AFTERGLOW SYNCHROTRON EMISSION

R.A.M.J. WIJERS¹ AND T.J. GALAMA²

SUBMITTED 26-MAY-98 to Astrophysical Journal

ABSTRACT

We have calculated synchrotron spectra of relativistic blast waves, and find predicted characteristic frequencies that are more than an order of magnitude different from previous calculations. For the case of an adiabatically expanding blast wave, which is applicable to observed gamma-ray burst (GRB) afterglows at late times, we give expressions to infer the physical properties of the afterglow from the measured spectral features.

We show that enough data exist for GRB 970508 to compute unambiguously the ambient density, $n = 0.04$, and the blast wave energy per unit solid angle, $\mathcal{E} = 4 \times 10^{52}$ erg/4 π sr. We also compute the energy density in electrons and magnetic field. We find that they are 13% and 7%, respectively, of the nucleon energy density and thus confirm for the first time that both are close to but below equipartition.

For GRB 971214, we show that the break found in its spectrum by Ramaprakash et al. (1998) is unlikely to be the synchrotron peak frequency, but could be the cooling break. We argue that the peak frequency was spotted in early IR measurements (Gorosabel et al. 1998). Using the three available constraints, we show that this afterglow has a lower energy, but the fractions transferred to electrons and magnetic field are consistent with those found in GRB 970508. The inferred gamma-ray to afterglow luminosity ratio is rather different between these two bursts, which we attribute to either intrinsic beaming of the gamma rays, or to a longer initial radiative phase in GRB 971214.

Subject headings: gamma rays: bursts — gamma rays: individual (GRB 970508) — gamma rays: individual (GRB 971214) — gamma rays: theory — acceleration of particles — magnetic fields

1. INTRODUCTION

Explosive models of gamma-ray bursts, in which relativistic ejecta radiate away some of their kinetic energy as they are slowed down by swept-up material, naturally lead to a gradual softening of the emission at late times. This late-time softer radiation has been dubbed the ‘afterglow’ of the burst, and its strength and time dependence were predicted theoretically (Mészáros and Rees, 1997). Soon after this prediction, the accurate location of GRB 970228 by the BeppoSAX satellite’s Wide Field Cameras (Piro et al. 1995, Jager et al. 1995) enabled the detection of the first X-ray and optical afterglow (Costa et al. 1997, Van Paradijs et al. 1997). Its behaviour agreed well with the simple predictions (Wijers et al. 1997, Waxman 1997a, Reichart 1997).

The basic model is a point explosion with an energy of order 10^{52} erg, which expands with high Lorentz factor into its surroundings. As the mass swept up by the explosion begins to be significant, it converts its kinetic energy to heat in a strong shock. The hot, shocked matter acquires embedded magnetic fields and accelerated electrons, which then produce the radiation we see via synchrotron emission. The phenomenon is thus very much the relativistic analogue of supernova remnant evolution, played out apparently in seconds due to the strong time contractions resulting from the high Lorentz factors involved. Naturally, the Lorentz factor of the blast wave decreases as more matter is swept up, and consequently the power output and typical energy decrease with time after the initial few seconds of gamma-ray emission. This produces the X-ray afterglows, which have been detected up to 10 days after the burst (Frontera et al. 1998), and the optical ones, which have been detected up to a year after the burst (Fruchter et al. 1997, Bloom et al. 1998, Castro-Tirado et al. 1998).

The burst of May 8, 1997, was bright for a relatively long time and produced emission from gamma rays to radio. This enabled a detailed analysis of the expected spectral features of a synchrotron spectrum, confirming in great detail that we are indeed seeing synchrotron emission, and that the dynamical evolution of the expanding blast wave agrees with predictions if the blast wave dynamics are adiabatic (Galama et al. 1998a,b). In principle, one can derive the blast wave properties from the observed synchrotron spectral features. The problem is that the characteristic synchrotron frequencies and fluxes are taken from simple dimensional analysis in the published literature, so they are not suitable for detailed data analysis. Since there are now enough data on the afterglows of a few GRBs to derive their physical properties, we amend this situation in Sect. 2, correcting the coefficients in the equations for the break frequencies by up to a factor 10. We then use our theoretical results to infer the physical properties of the afterglows of GRB 970508 (Sect. 3) and GRB 971214 (Sect. 4) and compare them. We conclude with a summary of results and venues for improved observations and analysis (Sect. 5).

¹Institute of Astronomy, Madingley Road, Cambridge CB3 0HA, UK

²Astronomical Institute ‘Anton Pannekoek’, University of Amsterdam, & Center for High Energy Astrophysics, Kruislaan 403, 1098 SJ Amsterdam, The Netherlands

2. RADIATION FROM AN ADIABATIC BLAST WAVE

2.1. Blast wave dynamics

We rederive the equations for synchrotron emission from a blast wave, to clean up some imprecisions in previous versions. Since the dynamical evolution of the blast waves should be close to adiabatic after the first hour or so, we specialise to the case of dynamically adiabatic evolution. This means that the radius r and Lorentz factor γ evolve with observer time as (Rees and Mészáros 1992, Mészáros and Rees 1997, Waxman 1997a, Wijers, Mészáros, and Rees 1997)

$$r(t) = r_{\text{dec}}(t/t_{\text{dec}})^{1/4} \quad (1)$$

$$\gamma(t) = \eta(t/t_{\text{dec}})^{-3/8}. \quad (2)$$

Here $\eta \equiv E/M_0c^2$ is the ratio of initial energy in the explosion to the rest mass energy of the baryons (mass M_0) entrained in it, the deceleration radius r_{dec} is the point where the energy in the hot, swept-up interstellar material equals that in the original explosion, and t_{dec} is the observer time at which the deceleration radius is reached. Denoting the ambient particle number density as n , we have

$$r_{\text{dec}} = \left(\frac{E}{4\pi\eta^2 n m_p c^2} \right)^{1/3} = 1.81 \times 10^{16} (E_{52}/n)^{1/3} \eta_{300}^{-2/3} \text{ cm} \quad (3)$$

$$t_{\text{dec}} = \frac{r_{\text{dec}}}{2\eta^2 c} = 3.35 (E_{52}/n)^{1/3} \eta_{300}^{-8/3} \text{ s}, \quad (4)$$

with m_p the proton mass and c the speed of light, and we have normalised to typical values: $E_{52} = E/10^{52}$ erg and $\eta_{300} = \eta/300$. Strictly speaking, we have defined n here as $n \equiv \rho/m_p$, where ρ is the ambient rest mass density. Setting $t_d = t/1$ day we then have, for $t > t_{\text{dec}}$,

$$r(t) = 2.29 \times 10^{17} (E_{52}/n)^{1/4} t_d^{1/4} \text{ cm} \quad (5)$$

$$\gamma(t) = 6.65 (E_{52}/n)^{1/8} t_d^{-3/8}. \quad (6)$$

Note that neither γ nor r depend on η : once the blast wave has entered its phase of self-similar deceleration, its initial conditions have been partly forgotten. The energy E denotes the initial blast wave energy; it and the ambient density do leave their marks. It should also be noted that these equations remain valid in an anisotropic blast wave, where the outflow is in cones of opening angle θ around some axis of symmetry, as long as its properties are uniform within the cone and the opening angle is greater than $1/\gamma$ (Rhoads 1998). We should then replace E by the equivalent energy per unit solid angle $\mathcal{E} \equiv E/\Omega$. To express this equivalence we shall write the normalisation for this case as $\mathcal{E}_{52} = \mathcal{E}/(4\pi/10^{52} \text{ erg})$, so we can directly replace E_{52} in all equations with \mathcal{E}_{52} to convert from the isotropic to the anisotropic case.

Before we can calculate the synchrotron emission from the blast wave, we have to compute the energies in electrons and magnetic field (or rather, summarise our ignorance in a few parameters). Firstly, we assume that electrons are accelerated to a power-law distribution of Lorentz factors, $P(\gamma_e) \propto \gamma_e^{-p}$, with some minimum Lorentz factor γ_m . We are ignorant of what p should be, but it can in practice be determined from the data. The total energy in the electrons is parameterised by the ratio, ϵ_e , of energy in electrons to energy in nucleons. This is often called the electron energy fraction, but that term is only appropriate in the limit of small ϵ_e . The post-shock nucleon energy is $\gamma m_p c^2$, and the ratio of nucleon to electron number densities will be the same as the pre-shock value, which we can parameterise as $2/(1+X)$, where X is the usual hydrogen mass fraction. In terms of these we have

$$\epsilon_e \equiv \frac{n_e \langle E_e \rangle}{n \gamma m_p c^2} = \frac{1+X}{2} \frac{m_e}{m_p} \frac{p-1}{p-2} \frac{\gamma_m}{\gamma} \quad (7)$$

$$\gamma_m = \frac{2}{1+X} \frac{m_p}{m_e} \frac{p-2}{p-1} \epsilon_e \gamma. \quad (8)$$

The strength of the magnetic field in the comoving frame is parameterised by setting the field energy density, $B'^2/8\pi$, to a constant fraction, ϵ_B , of the post-shock nucleon energy density $e' = 4\gamma^2 n m_p c^2$. (Primed quantities are measured in the rest frame of the shocked, swept-up material; others are measured in the frame of an observer outside the blast wave at rest relative to the explosion centre.) Consequently,

$$\begin{aligned} B' &= \gamma c \sqrt{32\pi n m_p \epsilon_B} \\ &= 2.58 \epsilon_B^{1/2} \mathcal{E}_{52}^{1/8} n^{3/8} t_d^{-3/8} \text{ G}. \end{aligned} \quad (9)$$

From the above relations, we can express the evolution of the synchrotron spectrum from the blast wave in terms of observable quantities and six unknown parameters: \mathcal{E}_{52} , n , X , p , ϵ_e , and ϵ_B . But first we need to relate the synchrotron spectrum to these parameters.

2.2. Synchrotron radiation

We now derive the correct synchrotron frequencies and fluxes for a uniform medium moving with a constant Lorentz factor relative to us. There are two corrections for realistic blast waves that we shall not apply: first, the blast wave is decelerating, which means that surfaces of constant arrival time are no longer the ideal ellipses expected for a constant speed of the blast wave (Rees 1966) and at a given time we see contribution from gas with different Lorentz factors. This effect has been discussed thoroughly (Waxman 1997b, Panaitescu & Mészáros 1998, Sari 1998). Also, it is usually assumed that the shocked radiating material moves towards us with uniform properties, but in reality the Lorentz factor varies from just behind the shock to the contact discontinuity. The density and other parameters vary accordingly (Blandford & McKee 1976). This effect has not yet been treated; it is expected to be comparable in importance to deceleration. Since both these effects are rather less important than our corrections to the synchrotron frequencies, we shall neglect both rather than attempt to apply only one of them. However, our improved treatment of the synchrotron emission is purely local and can be incorporated into any formalism that accounts for the varying local properties of the shocked medium at a fixed observer time.

We assume that the electron population in any local volume has an isotropic distribution of angles relative to the magnetic field, and that the magnetic field is sufficiently tangled that we may average the emission properties assuming a random mix of orientation angles between the field and our line of sight. The radiated power per electron per unit frequency, integrated over emission angles is

$$P'(\nu/\nu_{\perp}(\gamma_e), \alpha) = \frac{\sqrt{3}e^3 B' \sin \alpha}{m_e c^2} F\left(\frac{\nu}{\nu_{\perp} \sin \alpha}\right) \text{ erg cm}^{-2} \text{ s}^{-1} \text{ Hz}^{-1} \text{ electron}^{-1}, \quad (10)$$

where F is the standard synchrotron function (e.g., Rybicki & Lightman 1979), and e and m_e are the electron charge and mass. α is the angle between the electron velocity and the magnetic field, and

$$\nu_{\perp}(\gamma_e) = \frac{3\gamma_e^2 e B'}{4\pi m_e c}. \quad (11)$$

(i.e., the traditional characteristic synchrotron frequency equals $\nu_{\perp} \sin \alpha$ in our notation.) Next, we define the isotropic synchrotron function F_{iso} by averaging over an isotropic distribution of α . Setting $x_{\perp}(\gamma_e) = \nu/\nu_{\perp}(\gamma_e)$, we get

$$P'_{\text{iso}}(x_{\perp}) = \frac{\sqrt{3}e^3 B'}{m_e c^2} F_{\text{iso}}(x_{\perp}) \text{ erg cm}^{-2} \text{ s}^{-1} \text{ Hz}^{-1} \text{ electron}^{-1} \quad (12)$$

$$F_{\text{iso}}(x_{\perp}) = \int_0^{\pi/2} d\alpha \sin^2 \alpha F(x_{\perp}/\sin \alpha) \quad (13)$$

(We have made use of the symmetry of $\sin \alpha$ to absorb a factor 1/2 into confining the integral to the first quadrant. The apparent singularity at $\alpha = 0$ poses no problems because F decreases exponentially for large values of the argument.) Note that most calculations of blast wave spectra assume that the spectrum peaks at frequency $\gamma_e^2 e B'/m_e c$. Due to the neglect of the factor $3/4\pi$ and the fact that $F(x)$ peaks at $x = 0.28587$ and $F_{\text{iso}}(x)$ at $x = 0.22940$, this estimate leads to quite erroneous inferences about blast wave properties.

Finally, we must average the emission over a distribution of electron energies. We assume a simple power-law probability distribution of electrons between extreme values γ_m and γ_t :

$$f(\gamma_e) = \frac{f_0}{\gamma_m} \left(\frac{\gamma_e}{\gamma_m}\right)^{-p} \quad \gamma_m \leq \gamma_e \leq \gamma_t \quad (14)$$

$$f_0 = \frac{p-1}{1 - (\gamma_t/\gamma_m)^{1-p}} \quad (15)$$

Now let $x = \nu/\nu_{\perp}(\gamma_m)$. Then the average power per electron becomes

$$P'_{\text{PL}}(x) = \frac{\sqrt{3}e^3 B'}{m_e c^2} F_{\text{PL}}(x) \text{ erg cm}^{-2} \text{ s}^{-1} \text{ Hz}^{-1} \text{ electron}^{-1} \quad (16)$$

$$F_{\text{PL}}(x) = \frac{f_0}{2} x^{-\frac{p-1}{2}} \int_{x\gamma_m^2/\gamma_t^2}^x du u^{\frac{p-3}{2}} F_{\text{iso}}(u), \quad (17)$$

in which we have transformed integration variable from γ_e to $u \equiv x\gamma_m^2/\gamma_e^2$. The last equation shows the familiar result that for $1 \lesssim x \lesssim \gamma_t^2/\gamma_m^2$ the spectrum from a power law of electrons is itself a power law. Since this region is known to extend over many decades in GRB and afterglow spectra, we quote numerical results for the case $\gamma_t \gg \gamma_m$, for which the quoted results are independent of γ_t . The most easily identified point in the spectrum is its dimensionless maximum, x_p ,

and the dimensionless flux at this point, $F_{\text{PL}}(x_p) \equiv \phi_p$; their dependence on p is shown in Fig. 1. Both now depend on the electron energy slope p . This defines the first two numbers that we can measure in the spectrum:

$$\nu'_m = x_p \nu_{\perp}(\gamma_m) = \frac{3x_p}{4\pi} \frac{\gamma_m^2 e B'}{m_e c} \quad (18)$$

$$P'_{\nu_m} = \phi_p \frac{\sqrt{3} e^3 B'}{m_e c^2} \quad (19)$$

The calculation of the break frequency ν_c that separates radiation from slowly and rapidly cooling electrons (Sari, Piran, and Narayan 1998) is somewhat more difficult, because the cooling rate depends on both γ_e and pitch angle α . However, since the cooling and the emission are both dominated by $\alpha = \pi/2$, we may estimate the break as the peak of $F(x)$ for the value of γ_e where the cooling time for electrons with $\alpha = \pi/2$ equals the expansion time, t :

$$\gamma_c = \frac{6\pi m_e c}{\sigma_T \gamma B'^2 t} \quad (20)$$

$$\nu_c' = 0.286 \frac{3}{4\pi} \frac{\gamma_c^2 e B'}{m_e c} \quad (21)$$

In order to transform frequency and power from the rest frame of the emitting material to our frame, we note that the emission is isotropic in the rest frame by assumption. It is then trivial to compute the angle-average Doppler factors (see Rybicki & Lightman 1979, Ch.4). For the received power, we find $P = \gamma^2(1 + \beta^2/3)P'$, which we shall simplify to $P = 4\gamma^2 P'/3$ in keeping with the fact that our whole treatment is done in the ultrarelativistic limit, $\beta \rightarrow 1$. Similarly, the intensity-weighted mean change in any frequency is $\nu = 4\gamma\nu'/3$. Consequently, the appropriate mean of a power per unit frequency will transform as $P_{\nu} = \gamma P'_{\nu}$. Of course, the spectrum also gets broadened, but that will not affect the locus of characteristic frequencies significantly.

The synchrotron self-absorption frequency is usually set at the point where $\tau_{\nu} = 0.35$. Using the co-moving width of the shock, $\Delta r' = r/4\gamma$, and the expression for the synchrotron absorption coefficient (Rybicki & Lightman 1979), we get

$$\nu_a = 4\gamma\nu_a'/3 = 2.97 \times 10^8 \left(\frac{p+2}{p+3}\right)^{3/5} \frac{(p-1)^{8/5}}{p-2} (1+X)^{8/5} n^{3/5} \epsilon_e^{-1} \epsilon_B^{1/5} \mathcal{E}_{52}^{1/5} (1+z)^{-1} \text{ Hz} \quad (22)$$

where we have used equations 5–9 for the blast wave dynamics to express ν_a in terms of the unknowns we try to solve for, and added the correction for redshift, i.e. the equation in this form relates the observed frequency on Earth to the properties of the blast wave measured by a local observer at rest relative to the centre of the explosion. Note that the self-absorption frequency in this simplest form is time-independent. We now also translate the other two frequencies into practical form:

$$\nu_m = 4\gamma\nu_m'/3 = 5.73 \times 10^{16} x_p \left(\frac{p-2}{p-1}\right)^2 \epsilon_e^2 \epsilon_B^{1/2} \mathcal{E}_{52}^{1/2} (1+X)^{-2} (1+z)^{1/2} t_d^{-3/2} \text{ Hz} \quad (23)$$

$$\nu_c = 4\gamma\nu_c'/3 = 1.12 \times 10^{12} \epsilon_B^{-3/2} \mathcal{E}_{52}^{-1/2} n^{-1} (1+z)^{-1/2} t_d^{-1/2} \text{ Hz} \quad (24)$$

Note the non-trivial redshift dependence of both, which stems from the fact that t_d is also measured on Earth and therefore redshifted. The observed flux at ν_m can be obtained by noting that our assumption of uniformity of the shocked material means that all swept-up electrons since the start contribute the same average power per unit frequency at ν_m (at any frequency, in fact), which is given by Eq. (19). Adding one factor of γ to transform to the lab frame and accounting for the redshift, we have:

$$F_{\nu_m} = \frac{N_e \gamma P'_{\nu_m} (1+z)}{4\pi d_L^2}, \quad (25)$$

where N_e is the total number of swept-up electrons, related to the blast wave parameters by $N_e = \frac{4\pi}{3} r^3 n (1+X)/2$. The luminosity distance depends on cosmological parameters, and for an $\Omega = 1, \Lambda = 0$ universe, which we shall adopt here, is given by $d_L = 2c(1+z - \sqrt{1+z})/H_0$. Consequently,

$$F_{\nu_m} = 1.15 \frac{h_{70}^2}{(\sqrt{1+z} - 1)^2} \phi_p (1+X) \mathcal{E}_{52} n^{1/2} \epsilon_B^{1/2} \text{ mJy}, \quad (26)$$

where $h_{70} = H_0/70 \text{ km s}^{-1} \text{ Mpc}^{-1}$.

Equations 22, 23, 24, and 26 now are four independent relations between the four parameters of interest \mathcal{E}_{52} , n , ϵ_e , and ϵ_B . This means we can solve for all parameters of interest if we have measured all three break frequencies (not necessarily at the same time) and the peak flux of the afterglow. In addition this requires us to know the redshift of the burst, the electron index p , and the composition parameter, X , of the ambient medium. Note that multiple measurements of the same break at different times serve to test the model assumptions, but do not provide extra constraints on the parameters, since validity of the model implies that any of the four key equations is satisfied for all time if it is satisfied once. We

therefore define the constants $C_a \equiv \nu_a/\nu_{a*}$, $C_m \equiv \nu_m t_{\text{dm}}^{3/2}/\nu_{m*}$, $C_c \equiv \nu_c t_{\text{dc}}^{1/2}/\nu_{c*}$, and $C_F = F_{\nu_m}/F_{\nu_{m*}}$. Here starred symbols denote the numerical coefficients in each of the four equations, and times denote the time at which the quantity in question was measured. Rearranging the four equations then yields

$$\mathcal{E}_{52} = C_a^{-\frac{5}{6}} C_m^{-\frac{5}{12}} C_c^{\frac{1}{4}} C_F^{\frac{3}{2}} x_p^{\frac{5}{12}} \phi_p^{-\frac{3}{2}} (p-1)^{\frac{1}{2}} \left(\frac{p+2}{p+\frac{3}{2}}\right)^{\frac{1}{2}} (1+X)^{-1} (1+z)^{-\frac{1}{2}} \left(\frac{\sqrt{1+z}-1}{h_{70}}\right)^3 \quad (27)$$

$$\epsilon_e = C_a^{\frac{5}{6}} C_m^{\frac{11}{12}} C_c^{\frac{1}{4}} C_F^{-\frac{1}{2}} x_p^{-\frac{11}{12}} \phi_p^{\frac{1}{2}} \frac{(p-1)^{\frac{1}{2}}}{p-2} \left(\frac{p+2}{p+\frac{3}{2}}\right)^{-\frac{1}{2}} (1+X)(1+z)^{\frac{1}{2}} \left(\frac{\sqrt{1+z}-1}{h_{70}}\right)^{-1} \quad (28)$$

$$\epsilon_B = C_a^{-\frac{5}{2}} C_m^{-\frac{5}{4}} C_c^{-\frac{5}{4}} C_F^{\frac{1}{2}} x_p^{\frac{5}{4}} \phi_p^{-\frac{1}{2}} (p-1)^{\frac{3}{2}} \left(\frac{p+2}{p+\frac{3}{2}}\right)^{\frac{3}{2}} (1+X)(1+z)^{-\frac{5}{2}} \left(\frac{\sqrt{1+z}-1}{h_{70}}\right) \quad (29)$$

$$n = C_a^{\frac{25}{6}} C_m^{\frac{25}{12}} C_c^{\frac{3}{4}} C_F^{-\frac{3}{2}} x_p^{-\frac{25}{12}} \phi_p^{\frac{3}{2}} (p-1)^{-\frac{5}{2}} \left(\frac{p+2}{p+\frac{3}{2}}\right)^{-\frac{5}{2}} (1+X)^{-1} (1+z)^{\frac{7}{2}} \left(\frac{\sqrt{1+z}-1}{h_{70}}\right)^{-3} \quad (30)$$

The last factor in each of these stems from the specific cosmological model adopted, and has entered the solution only via Eq. (25). To generalise to any cosmology, all that is needed is to replace $(\sqrt{1+z}-1)/h_{70}$ in the above equations by $(d_L/8.57 \text{ Gpc})/\sqrt{1+z}$.

3. OBSERVED AND INFERRED PARAMETERS OF GRB 970508

GRB970508 was a moderately bright γ -ray burst (Costa et al. 1997, Kouveliotou et al. 1997). It was detected on May 8.904 UT with the Gamma-Ray Burst Monitor (GRBM; Frontera et al. 1991), and with the Wide Field Cameras (WFCs; Jager et al. 1995) on board the Italian-Dutch X-ray observatory BeppoSAX (Piro, Scarsi, & Butler 1995). Optical observations of the WFC error box (Heise et al. 1997), made on May 9 and 10, revealed a variable object at RA = $06^{\text{h}}53^{\text{m}}49^{\text{s}}.2$, Dec = $+79^{\circ}16'19''$ (J2000), which showed an increase by ~ 1 mag in the V band (Bond 1997). BeppoSAX Narrow Field Instrument observations revealed an X-ray transient (Piro et al. 1997) whose position is consistent with that of the optical variable, and Frail et al. (1997) found the first GRB radio afterglow for GRB 970508; the radio source position coincides with that of the optical source (Bond 1997).

The spectrum of the optical variable showed absorption lines at redshifts 0.77 and 0.835, indicating that 0.835 is the minimum redshift of the afterglow (Metzger et al. 1997). Subsequently, an [O II] emission line with $z = 0.835$ was also found in the spectrum (Metzger et al. 1997), which is often associated with star forming regions in galaxies. A faint underlying galaxy or star forming region is inferred to indeed exist from a levelling off of the light curve after 6–11 months (Bloom et al. 1998, Castro-Tirado et al. 1998). It must be very compact, since the HST limits on an extended object underlying the GRB are fainter than the magnitude inferred from the light curve (Fruchter 1998). It is therefore almost certain that the compact nebula is the source of the [O II] line, and therefore also of the majority of the absorption lines. Given its compactness, a chance location of the burst far behind it is unlikely, and we shall assume that the burst occurred in this nebula, i.e. its redshift is 0.835.

From the light curve behaviour and broad-band spectrum (Fig. 2) of GRB 970508, Galama et al. (1998a,b) deduced the other properties of the burst required to calculate the physical parameters of the afterglow. We summarise them here: at $t = 12.1$ d after trigger, the break frequencies are $\nu_a = 2.5 \times 10^9$ Hz, $\nu_m = 8.6 \times 10^{10}$ Hz, and $\nu_c = 1.6 \times 10^{14}$ Hz. The peak flux is $F_{\nu_m} = 1.7$ mJy and the electron index $p = 2.2$. After the first 500 s electrons no longer cooled efficiently and the afterglow must evolve adiabatically. We shall set the cosmological parameters to be $\Omega = 1$, $\Lambda = 0$, $H_0 = 70$ km s $^{-1}$ Mpc $^{-1}$. As noted above, they only enter the solution via the luminosity distance, and alternatives can therefore be incorporated easily via the substitution given below Eq. (30). Finally, we adopt $X = 0.7$ for the composition of the ambient medium. There are no reasons in the model to assume the ambient medium would not have normal cosmic abundance. While the metallicity Z is a strong function of redshift, X is hardly redshift-dependent, since the balance between H and He in cosmic matter has not been changed very much by nucleosynthesis. Using further that $x_{2.2} = 0.580$, $\phi_{2.2} = 0.611$, we find

$$\begin{aligned} \mathcal{E}_{52} &= 3.7 & n &= 0.035 \\ \epsilon_e &= 0.13 & \epsilon_B &= 0.068. \end{aligned} \quad (31)$$

We do note once more our deliberate use of \mathcal{E}_{52} , the energy per unit solid angle scaled to that of an isotropic explosion of 10^{52} erg, in stead of the total energy: \mathcal{E}_{52} is truly constrained by the data, whereas the total energy requires us to know the as yet poorly constrained beaming of bursts. Our value of \mathcal{E}_{52} does clearly rule out the very high energy estimates by Brainerd (1998) from the radio data alone. We have demonstrated for the first time that the electron and magnetic field energy densities are indeed close to but somewhat below equipartition value. The ambient density is on the low side of normal for a disc of a galaxy but definitely higher than expected for a halo, lending further support to the notion that bursts occur in gas-rich environments. As an aside, we note that switching the values of ν_m and ν_c , which is allowed by the shape of the spectrum at 12.1 d, does not give a sensible solution (e.g., $\epsilon_e = 20$.) This confirms the choice of Galama et al. (1998b), who noted that this solution was not compatible with the temporal evolution of the afterglow.

The gamma-ray fluence of GRB 970508 was measured with BATSE to be $(3.1 \pm 0.2) \times 10^{-6}$ erg cm $^{-2}$. Using $z = 0.835$ and $h_{70} = 1$, this implies $\mathcal{E}_{52\gamma} = 0.63$. In other words, the energy emitted in gamma rays is 17% of the total blast wave

energy (per unit solid angle in our direction). According to Galama et al. (1998b), the afterglow was cooling efficiently until 500s after trigger; this means that during the gamma-ray phase all the energy given to electrons would be radiated away quickly, and mostly in gamma rays. If this phase is not too long, the energy radiated in gamma rays should be $\mathcal{E}_{52\gamma} = \epsilon_{e\gamma}\mathcal{E}_{52i}$, where $\epsilon_{e\gamma}$ is the value of ϵ_e during the early, gamma-ray emitting phase and \mathcal{E}_{52i} is the initial value of \mathcal{E}_{52} . Since the subsequent phase will be adiabatic, the blast wave energy measured at late times should be $\mathcal{E}_{52} = (1 - \epsilon_{e\gamma})\mathcal{E}_{52i}$. Eliminating the initial energy, we conclude that

$$\frac{\epsilon_{e\gamma}}{1 - \epsilon_{e\gamma}} = \frac{\mathcal{E}_{52\gamma}}{\mathcal{E}_{52}}. \quad (32)$$

Therefore the measured ratio of gamma-ray fluence to late time blast wave energy implies that $\epsilon_{e\gamma} = 0.15$, or slightly greater if some of the initial energy output is at $E < 20$ keV. Compared with $\epsilon_e = 0.13$ at late times, this demonstrates the near-constancy of the fraction of energy that is given to the electrons. Since the inferences about the initial gamma-ray fluence are independent of the whole machinery on blast wave synchrotron emission in the previous section, we may view this agreement as modest evidence that the coefficients derived there are close to correct, despite our simplification of the dynamics.

It is also interesting to compare the properties at late times with those derived from radio observations. The scintillation size after 1 month is about 10^{17} cm (Frail et al. 1997), whereas our formulae give a transverse size of 3×10^{17} cm, in reasonable agreement given the statistical nature of the scintillation size and our neglect of the gradients in properties in the transverse direction, to which this particular measurement is of course sensitive. The Lorentz factor at this time is 3.3, so the evolution is still just in the ultrarelativistic regime. The field at this time is $B' = 0.06$ G. Katz and Piran (1997) estimated a size of the afterglow of GRB 970508 from a crude measurement of the self-absorption frequency. They found a size of 10^{17} cm, and assuming an ambient density of 1 cm^{-3} they found that the Lorentz factor had already decreased to 2, and that most of the energy of the blast wave had been lost, i.e. it had evolved with radiative dynamics. The numbers we derive from our full solution after 1 week are: $\gamma = 6.5$, $r = 2 \times 10^{17}$ cm. This means the blast wave is still quite relativistic, and with our low ambient density there is no need for radiative evolution.

4. PROPERTIES OF GRB 971214

This burst occurred on 1997 December 14.9727 UT. With a fluence of $1.1 \times 10^{-5} \text{ erg cm}^{-2}$ it is a moderately bright burst (Kippen et al. 1997). After localisation by the BeppoSAX Wide Field Camera in X rays (Heise et al. 1997), the optical afterglow of this burst was found by Halpern et al. (1998). It shows evidence of strong reddening (Halpern et al. 1998, Ramaprakash et al. 1998). Once the afterglow had faded, a host galaxy became visible underneath it and its redshift was measured to be 3.42 (Kulkarni et al. 1998).

Ramaprakash et al. (1998) noted a break in the spectrum of the afterglow at 3×10^{14} Hz, 0.58 days after trigger, which they interpreted as the peak frequency ν_m . The exponent of the power-law decay of the flux at V , R , and I band is reported to be 1.2 ± 0.2 by Kulkarni et al. (1998) and 1.4 ± 0.2 by Halpern et al. (1998). We shall adopt the value 1.3 ± 0.2 in this paper. For the simple adiabatic model used by Ramaprakash et al., this implies $p = 2.7$, so using Eq. (23) we have

$$\mathcal{E}_{52} = 21 \frac{2}{1+z} \left(\frac{\epsilon_e}{0.2}\right)^{-4} \left(\frac{\epsilon_B}{0.1}\right)^{-1}. \quad (33)$$

The coefficient is 50 times larger than in eq.3 of Ramaprakash et al., almost solely due to our more accurate calculation of the peak frequency. We are somewhat doubtful, however, that this calculation is relevant here. If the break is indeed the peak frequency, then the peak flux is $14 \mu\text{Jy}$ (corrected for absorption). We then use Eq. (26) to derive an independent estimate of the blast wave energy from this peak flux:

$$\mathcal{E}_{52} = 0.043n^{-1/2} \left(\frac{\epsilon_B}{0.1}\right)^{-1/2} \quad (34)$$

This value is difficult to reconcile with the energy estimate from ν_m , so we reject the possibility that this break is ν_m .

However, we do believe that the passing of ν_m has been spotted in this afterglow, thanks to early K band measurements by Gorosabel et al. (1998) 3–5 hours after trigger. In Fig. 3 we show these data combined with a measurement after 14 hours (Ramaprakash et al. 1998). The data are not strongly inconsistent with a pure power law fit ($\chi^2/\text{dof}=2.0$), but are strongly suggestive of a break passing through K after about 5 hours. Using the factor 1.4 extinction at K derived by Ramaprakash et al. (1998) combined with the measured $K = 18$ after 5 hours, this implies $F_{\nu_m} = 58 \mu\text{Jy}$. We can then again use equations 23 and 26 to get two expressions for the energy in terms of the other unknowns:

$$\mathcal{E}_{52} = 4.5 \left(\frac{\epsilon_e}{0.13}\right)^{-4} \left(\frac{\epsilon_B}{0.068}\right)^{-1} \quad (35)$$

$$\mathcal{E}_{52} = 1.1 \left(\frac{n}{0.035}\right)^{-1/2} \left(\frac{\epsilon_B}{0.068}\right)^{-1/2} \quad (36)$$

Here we have scaled the unknowns to the values found for GRB 970508. For ϵ_B and ϵ_e that may be justified, since they are presumably set by the microphysics behind ultrarelativistic shocks. There is obviously no reason why n should be

the same, but the consistency of the energy values derived from two independently measured quantities supports our identification of the synchrotron peak.

This leaves us with the break observed by Ramaprakash et al. (1998) around 1 micron (3×10^{14} Hz) after 0.58 d. A complication may be that there is definite dust extinction of the afterglow within the host, and that the 2200 Å dust absorption bump redshifted to $z = 3.42$ would lie at precisely 1 micron. However, in low-metallicity environments this bump is often absent, so depending on how much star formation has happened in the region where the burst went off, we may or may not expect it here. Let us assume that it is absent, so that the break is intrinsic to the burst. Ramaprakash et al. reject the possibility that the break is the cooling frequency ν_c , on the grounds that the expected change of slope at this point is only 0.5, and the break is sharper than that. However, the sharpness of the break is greatly increased by the dust extinction correction, because that is stronger at the shortest wavelengths (see their Fig.2). The amount of dust extinction they find is based on the assumed intrinsic spectral slope. Their reasoning is as follows: afterglow light curves scale as $F(\nu, t) \propto \nu^{-\beta} t^{-\delta}$, where β is a function of δ for a given model. The simplest adiabatic model with slowly cooling electrons gives $\beta = 2\delta/3$ (e.g. Wijers et al. 1997), therefore they infer from the observed $\delta = 1.2$ that the spectral slope β must equal 0.8. The observed slope is much steeper, and only one value of dust extinction will bring the two into agreement, which fixes the amount of extinction. The extinction-corrected spectrum indeed shows a fairly sharp break. The problem is that this reasoning partly pre-empts the result. Let us assume instead that the break is ν_c . Then the electrons that radiate in the *VRI* bands used in the argument are above the cooling break, which means that the relation between β and δ is different: $\beta = (2\delta + 1)/3$ (Sari et al. 1998). Using our value of δ (1.3) we expect a steeper intrinsic slope in *VRI* of 1.2, reducing the inferred amount of extinction and the strength of the break. The procedure is illustrated in Fig. 4: the spectrum is consistent with a slope change of 0.5 expected at ν_c , if we choose $\nu_c = 4 \times 10^{14}$ Hz. The *K* flux admittedly deviates somewhat from this model, but scarcely by more than 1σ . Combined with the fact that a better candidate for the passage of ν_m is available, we conclude that the break seen by Ramaprakash et al. is ν_c . Incidentally, the amount of extinction, 1.2 mag at a rest frame wavelength of 1250 Å, is very modest and does not imply a special location of the burst within the galaxy.

Now that we identified all but the self-absorption frequency in the afterglow of GRB 971214, we may use equations 27–30 to get all the parameters of the burst, leaving their dependence on the unknown ν_a explicit. But the numbers become somewhat different from those above. First, in our interpretation the optical decay curves are in the fast electron cooling regime, hence the value of p changes to $p = (4\delta + 2)/3 = 2.4$ (Sari, Piran, and Narayan 1998). The peak frequency $\nu_m = 1.4 \times 10^{14}$ Hz at 0.167 days. The peak flux is somewhat reduced, since the extinction correction is less: $F_{\nu_m} = 56 \mu\text{Jy}$. The cooling frequency is $\nu_c = 4 \times 10^{14}$ Hz at 0.52 days. It follows that

$$\begin{aligned} \mathcal{E}_{52} &= 0.53 \nu_{a,\text{GHz}}^{-5/6} \quad n = 0.37 \nu_{a,\text{GHz}}^{25/6} \\ \epsilon_e &= 0.20 \nu_{a,\text{GHz}}^{5/6} \quad \epsilon_B = 0.031 \nu_{a,\text{GHz}}^{-5/2}. \end{aligned} \quad (37)$$

Since ϵ_B may be a universal parameter because it is determined by microphysics behind the shock, we can try to force it to same value, $\epsilon_B = 0.068$, as for GRB 970508. This implies $\nu_a = 0.73$ GHz, which then leads to $\epsilon_e = 0.16$. It is encouraging that the assumption of universality of ϵ_B also leads to nearly the same value for ϵ_e for the two bursts, since that should also be set by microphysics behind the shock. The ambient density then becomes $n = 0.10$, higher than for GRB 970508 and more typical of a location in a gaseous disc of a galaxy. The energy, at $\mathcal{E}_{52} = 0.68$, is now significantly less than for GRB 970508. Since the radio fluxes are proportional to the energy, the lower energy and greater distance may explain the absence of a radio afterglow for this burst.

The available data on GRB 971214 paint a picture of this afterglow that is similar in many ways to the one for GRB 970508. The main difference lies in the optical to gamma-ray flux ratio. For GRB 970508, the initial gamma-ray flux at 100 keV is about 20% of the measured F_{ν_m} for the afterglow; for GRB 971214 the initial gamma-ray flux exceeds F_{ν_m} of the afterglow by a factor 10, and so $\mathcal{E}_{52\gamma} \gg \mathcal{E}_{52}$. There are many possible interpretations for this. It may indicate that the bursts differ intrinsically in how strong the radiative losses at early times are. For GRB 970508, the efficient electron cooling phase ended around 500 s after trigger (i.e. at that time $\nu_m = \nu_c$; Galama et al. 1998b). For GRB 971214, the same extrapolation of ν_c and ν_m shows that the efficient electron cooling phase lasted until 3000 s. This means GRB 971214 could have been much more strongly radiative during its gamma-ray phase, which may be the cause of both the higher initial gamma-ray flux and the lower blast wave energy at late times. The difference could also be a beaming effect: the gamma-ray emission from a burst, coming from the fastest material, could well be significantly beamed. Since a realistic beam is likely to be most powerful in the centre and weaker towards the edges, it could simply be that GRB 971214 was aimed more precisely at us.

5. CONCLUSION

We have calculated the synchrotron spectra from the blast waves causing GRB afterglows and derive more accurate expressions for the relation between measured break frequencies and the intrinsic properties of the blast wave. These allow us to relate the blast wave properties to observable quantities more accurately. We correct the expression for the blast wave energy by almost two orders of magnitude. Our expressions are exact for an undecelerated, uniform medium. Deceleration and radial structure of the shock are expected to change the expressions for the final parameters by another factor few, much less than the corrections found here but still of interest.

There is enough data on GRB 970508 to compute all intrinsic parameters of the blast wave. The energy in the blast

wave is 4×10^{52} erg/ 4π sterad; since the beaming of the burst is not very well constrained, the total energy may be as low as 10^{51} erg. The ambient density into which the blast wave expands is 0.04 cm^{-3} , on the low side for a disc of a galaxy. The fraction of post-shock energy that goes into electrons is 13%, and that into field, 7%. We also estimate the fraction of energy transferred to electrons during the gamma-ray phase, and find this to be 15%. The agreement with the later blast wave value shows that the fraction of energy given to electrons is constant from 10 s to 10^6 s after the trigger.

For GRB 971214 we lack the self-absorption frequency, and compute the properties with this missing frequency left as a parameter. It is striking that if we choose the self-absorption frequency such that the magnetic-field equipartition fraction equals the value found for GRB 970508, then the electron energy fraction becomes almost equal to the value for GRB 970508. This supports the hypothesis that the magnetic field and electron energy densities are universal parameters. The blast wave energy per unit solid angle was 5 times greater in GRB 970508. More definite statements about universality of properties obviously has to await a larger sample of well-analysed afterglows.

A distinct difference between the two afterglows is that GRB 970508 emitted a gamma-ray energy per unit solid angle that was only 17% of the energy per unit solid angle in the blast wave, whereas in GRB 971214 it was 40 times the blast wave energy per unit solid angle. The difference could be caused by a longer initial radiative phase in GRB 971214, causing it to emit more of the initial explosion energy in gamma rays and leaving less for the adiabatic blast wave phase. On the other hand, since gamma-ray bursts are probably powered by deep gravitational collapses, which due to angular momentum conservation will almost certainly produce rapidly spinning remnants, it is quite likely that GRB explosions are beamed, and that this beaming is stronger in gamma rays than in optical, because the former come from the fastest ejecta near the rotation axis. The energy per unit solid angle in the afterglow could then simply be small because it is an average over the much larger solid angle subtended by the material that emits the optical radiation.

Our analysis emphasises the importance of early measurements covering a wide range of wavelengths. The full identification of the cooling frequency ν_c in GRB 970508 hinged on abundant photometry, including colours, being available from 0.5 days after the burst, since the break passed R after 1.5 days (Galama et al. 1998b). In H and K , the action lasted a week (Galama et al. 1998b), and this is the general trend: there is more time in IR, since all breaks pass later there. However, our revised coefficient for the peak frequency, ν_m , shows that this can be caught only in the IR and even then within hours of the trigger. A case in point are the very early K' band measurements of GRB 971214 by Gorosabel et al. (1998), which provide an invaluable constraint on this afterglow as they just caught the passage of ν_m through K' . Therefore, we encourage first and foremost early long-wavelength coverage, including searches for afterglows in IR, as a method of effectively constraining afterglow parameters. Two of the three crucial frequencies in an afterglow pass the optical and IR within hours and days, respectively. There is no time to first search and only then attempt broad coverage.

R.A.M.J. Wijers is supported by a Royal Society URF grant. T.J. Galama is supported through a grant from NFRA under contract 781.76.011.

REFERENCES

- Blandford, R. D. and McKee, C. F.: 1976, *Phys. Fluids* **19**, 1130
 Bloom, J. S., Kulkarni, S. R., Djorgovski, S. G., and Frail, D. A.: 1998, *GCN Circ.* 30
 Bond, H. E.: 1997, *IAU Circ.* 6654
 Brainerd, J. J.: 1998, *ApJ* **496**, L67–L70
 Castro-Tirado, A. J., Gorosabel, J., Galama, T., Groot, P., van Paradijs, J., and Kouveliotou, C.: 1998, *IAU Circ.* 6848
 Costa, E., Feroci, M., Piro, L., Soffitta, P., Cinti, M. N., Frontera, F., Zavattini, G., Nicastro, L., Palazzi, E., Tesserì, A., Gandolfi, G., Smith, M., Ricci, R., Coletta, A., Heise, J., in 't Zand, J., and Tavani, M.: 1997a, *IAU Circ.* 6649
 Costa, E., Frontera, F., Heise, J., Feroci, M., in 't Zand, J., Fiore, F., Cinti, M. N., Dal Fiume, D., Nicastro, L., Orlandini, M., Palazzi, E., Rapisarda, M., Zavattini, G., Jager, R., Parmar, A., Owens, A., Molendi, S., Cusumano, G., Maccarone, M. C., Giarrusso, S., Coletta, A., Antonelli, L. A., Giommi, P., Muller, J. M., Piro, L., and Butler, R. C.: 1997b, *Nature* **387**, 783–785
 Frail, D. A., Kulkarni, S. R., Nicastro, L., Feroci, M., and Taylor, G. B.: 1997, *Nature* **389**, 261
 Frontera, F. and et al.: 1991, *Adv. Space Res.* **11**, 281
 Frontera, F., Greiner, J., Antonelli, L. A., Costa, E., Fiore, F., Parmar, A. N., Piro, L., Boller, T., and Voges, W.: 1998, *A&A in press*, (astro-ph/9804270)
 Fruchter, A., Livio, M., Macchetto, D., Petro, L., Sahu, K., Pian, E., Frontera, F., Thorsett, S., and Tavani, M.: 1997, *IAU Circ.* 6747
 Fruchter, A. S.: 1998, in C. Meegan, R. Preece, and T. Koshut (eds.), *Fourth Huntsville Gamma-ray Burst Symposium*
 Galama, T. J., Wijers, R. A. M. J., Bremer, M., Groot, P. J., Strom, R. G., de Bruyn, A. G., Kouveliotou, C., Robinson, C. R., and van Paradijs, J.: 1998a, *ApJ in press*, (astro-ph/9804190)
 Galama, T. J., Wijers, R. A. M. J., Bremer, M., Groot, P. J., Strom, R. G., Kouveliotou, C., and van Paradijs, J.: 1998b, *ApJ in press*, (astro-ph/9804191)
 Garcia, M. R., Muench, A., Tollestrup, E., Callanan, P. J., and McCarthy, J.: 1997, *IAU Circ.* 6792
 Gorosabel, J., Castro-Tirado, A. J., Willott, C. J., Hippelein, H., Greiner, J., Shlyapnikov, A., Guziy, S., Costa, E., Feroci, M., Frontera, F., Nicastro, L., and Palazzi, E.: 1998, *A&A in press*
 Halpern, J. P., Thorstensen, J. R., Helfand, D. J., and Costa, E.: 1998, *Nature* **393**, 41–43
 Heise, J., in 't Zand, J., Costa, E., Feroci, M., Piro, L., Soffitta, P., Amati, L., Cinti, M. N., Frontera, F., Zavattini, G., Nicastro, L., Palazzi, E., Tesserì, A., Gandolfi, G., Smith, M., Muller, H., Ricci, D., Coletta, A., and Tavani, M.: 1997a, *IAU Circ.* 6654
 Heise, J., in 't Zand, J., Spoliti, G., Torroni, V., Ricci, D., Piro, L., Costa, E., Feroci, M., and Frontera, F.: 1997b, *IAU Circ.* 6787
 Jager, R., Heise, J., in 't Zand, J., and Brinkman, A. C.: 1995, *Adv. Space Res.* **13**, 315–318
 Katz, J. I. and Piran, T.: 1997, *ApJ* **490**, 772
 Kippen, M. R., Woods, P., Connaughton, V., Smith, D. A., Levine, A. M., and Hurley, K.: 1997, *IAU Circ.* 6789
 Kouveliotou, C., Briggs, M. S., Preece, R., Fishman, G. J., Meegan, C. A., and Harmon, B. A.: 1997, *IAU Circ.* 6660
 Kulkarni, S. R., Djorgovski, S. G., Ramaprakash, A. N., Goodrich, R., Bloom, J. S., Adelberger, K. L., Kundic, T., Lubin, L., Frail, D. A., Frontera, F., Nicastro, L., Barth, A. J., Davis, M., Filippenko, A. V., and Newman, J.: 1998, *Nature* **393**, 35–39
 Mészáros, P. and Rees, M. J.: 1997, *ApJ* **476**, 232–237
 Metzger, M. R., Cohen, J. G., Chaffee, F. H., and Blandford, R. D.: 1997a, *IAU Circ.* 6676
 Metzger, M. R., Djorgovski, S. G., Kulkarni, S. R., Steidel, C. C., Adelberger, K. L., Frail, D. A., Costa, E., and Frontera, F.: 1997b, *Nature* **387**, 879
 Panaitescu, A. and Mészáros, P.: 1998, *ApJ* **493**, L31–L34
 Piro, L., Costa, E., Feroci, M., Soffitta, P., Antonelli, L. A., Fiore, F., Giommi, P., Owens, A., Parmar, A., Molendi, S., Cusumano, G., in 't Zand, J., Heise, J., Frontera, F., Zavattini, G., Nicastro, L., Palazzi, E., Smith, M., Gandolfi, G., Torroni, V., Spoliti, G., Coletta, A., Capalbi, M., Rebecchi, S., Ricci, D., Bruca, L., Crisigiovanni, G., Salotti, L., Gennaro, G., DeLibero, C., and Butler, R. C.: 1997, *IAU Circ.* 6656
 Piro, L., Scarsi, L., and Butler, R. C.: 1995, *Proc. SPIE* **2517**, 169–181

- Ramaprakash, A. N., Kulkarni, S. R., Frail, D. A., Koresko, C., Kuchner, M., Goodrich, R., Neugebauer, G., Murphy, T., Eikenberry, S., Bloom, J. S., Djorgovski, S. G., Waxman, E., Frontera, F., Feroci, M., and Nicastro, L.: 1998, *Nature* **393**, 43–46
- Rees, M. J.: 1966, *Nature* **211**, 468–470
- Rees, M. J. and Mészáros, P.: 1992, *MNRAS* **258**, L41–L43
- Reichart, D. E.: 1997, *ApJ* **485**, L57–L60
- Rhoads, J. E.: 1998, *ApJ* submitted
- Rybicki, G. B. and Lightman, A. P.: 1979, John Wiley & Sons, New York
- Sari, R.: 1998, *ApJ* **494**, L49–L52
- Sari, R., Piran, T., and Narayan, R.: 1998, *ApJ* **submitted**, (astro-ph/9712005)
- Tanvir, N., Wyse, R., Gilmore, G., and Corson, C.: 1997, *IAU Circ.* 6796
- van Paradijs, J., Groot, P. J., Galama, T., Kouveliotou, C., Strom, R. G., Telting, J., Rutten, R. G. M., Fishman, G. J., Meegan, C. A., Pettini, M., Tanvir, N., Bloom, J., Pedersen, H., Noerdgaard-Nielsen, H. U., Linden-Voernle, M., Melnick, J., van der Steene, G., Bremer, M., Naber, R., Heise, J., in 't Zand, J., Costa, E., Feroci, M., Piro, L., Frontera, F., Zavattini, G., Nicastro, L., Palazzi, E., Hanlon, L., and Bennett, K.: 1997, *Nature* **386**, 686
- Waxman, E.: 1997a, *ApJ* **491**, L19–L22
- Waxman, E.: 1997b, *ApJ* **485**, L5–L8
- Wijers, R. A. M. J., Rees, M. J., and Mészáros, P.: 1997, *MNRAS* **288**, L51–L56

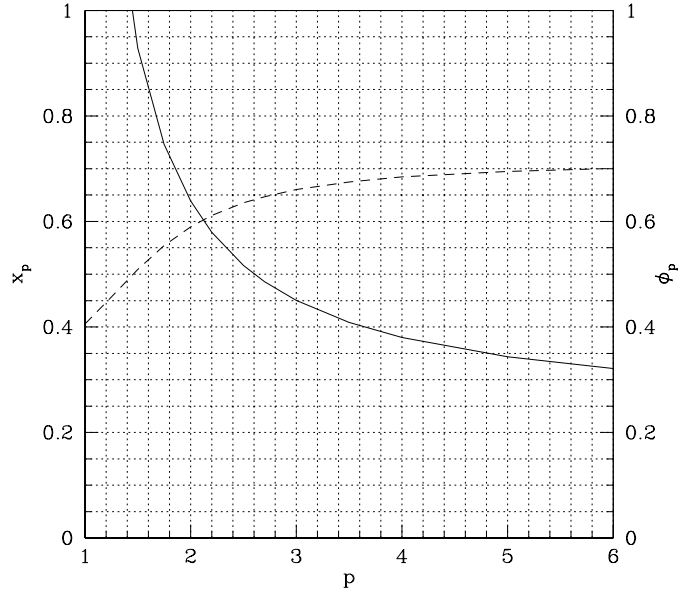


FIG. 1.— The dimensionless location x_p (solid) and dimensionless peak flux ϕ_p (dashed) of a synchrotron spectrum from a power law of electrons, as a function of the power law index, p of the electron energy distribution.

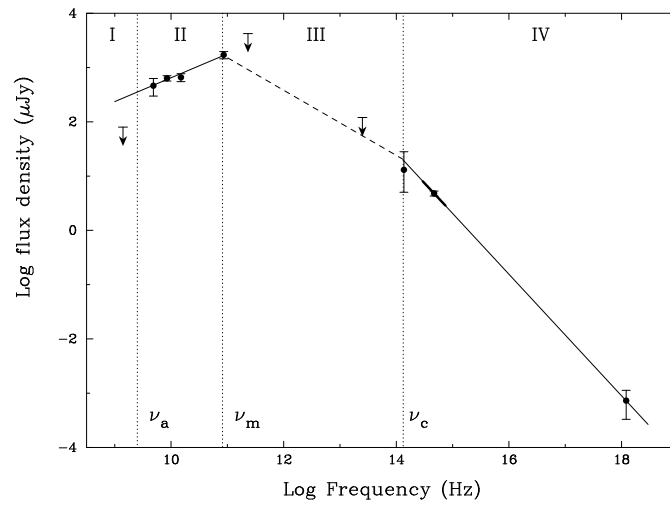


FIG. 2.— The X-ray to radio spectrum of GRB 970508 on May 21.0 UT (12.1 days after the event) from Galama et al. (1998b). Indicated are the inferred values of the break frequencies ν_a , ν_m and ν_c for May 21.0 UT.

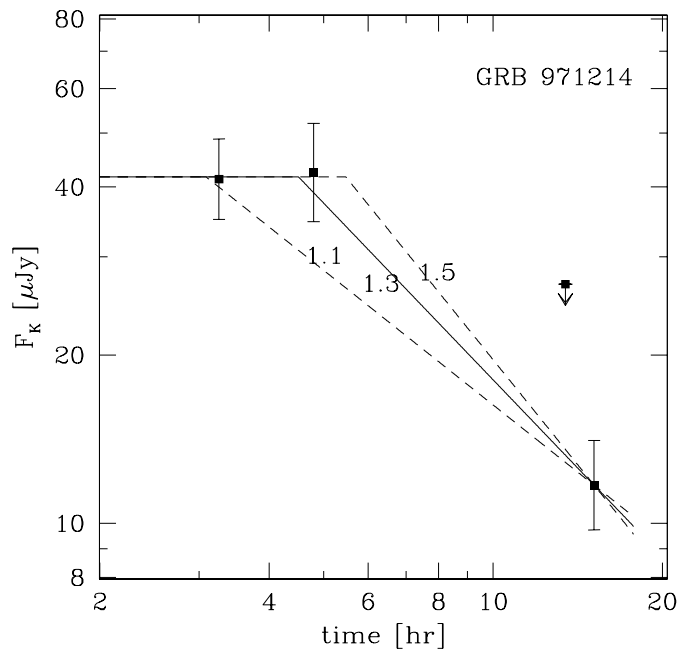


FIG. 3.— The K flux of GRB971214 as a function of time. Extrapolations to early times of the Keck measurement after 14 hours (Kulkarni et al. 1998) are shown for the same three values of δ used in Fig. 4. Other data are by Gorosabel et al. (1998) and Garcia et al. 91998; the upper limit). Note that the actual slope of each curve is 0.25 less than the value of δ (by which it is labelled) because K lies below the cooling break, where the temporal slope is always less steep by $1/4$ than above it.

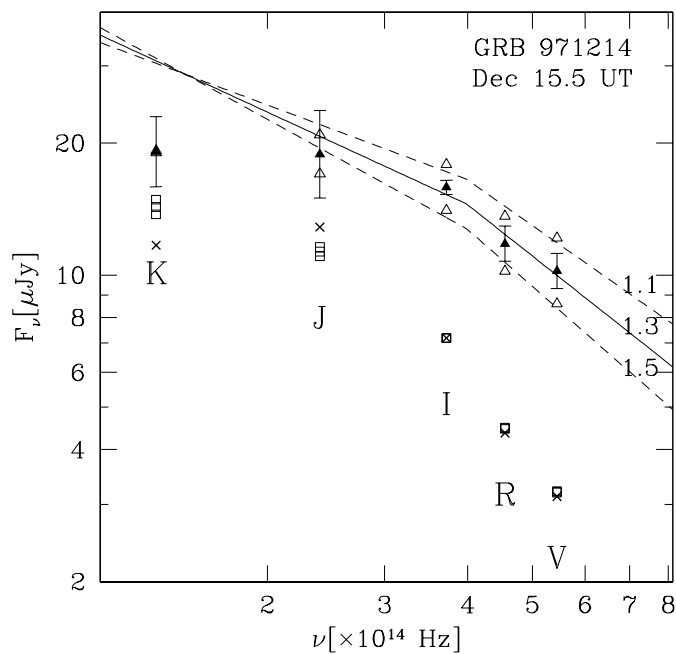


FIG. 4.— The intrinsic spectrum of GRB971214 on 1997 Dec 15.5 UT. Crosses indicate the measured fluxes, and squares the values extrapolated to Dec 15.5 UT (the epoch of the I data point). Three values of the temporal decay exponent δ above the break (i.e. for the V and R data) were used: 1.1, 1.3, and 1.5. The best-fit dereddened data are shown for each case (solid triangles for the central value, open triangles for the others). The best-fit broken power law spectra are labelled with the value of δ for which they are derived. The slopes above the break for the three spectra are 1.07, 1.2, and 1.33, respectively, and 0.5 less in each case below the break. (The error bars apply to all points at a given band, but are only shown once for clarity; note that the J error is much larger than that used by Ramaprakash et al. (1998), in agreement with the original report (Tanvir et al. 1997)).